

## 6. HIGH-RESOLUTION CARBONATE CONTENT ESTIMATED FROM DIFFUSE SPECTRAL REFLECTANCE FOR LEG 172 SITES<sup>1</sup>

Liviu Giosan,<sup>2</sup> Roger D. Flood,<sup>2</sup> Jens Grützner,<sup>3</sup>  
Sven-Oliver Franz,<sup>3</sup> Maria-Serena Poli,<sup>4</sup> and Sveinung Hagen<sup>5</sup>

### ABSTRACT

Visual-domain diffuse reflectance data collected aboard the *JOIDES Resolution* with the Minolta spectrometer CM-2002 during Ocean Drilling Program Leg 172 have been used to estimate successfully the carbonate content of sediments. Calibration equations were developed for each site and for each lithostratigraphic unit (or subunit at Site 1063) using multiple linear regression on raw as well as pretreated reflectance spectra (i.e., first-order derivation and squaring of raw reflectance spectra) for a total of 4141 direct carbonate measurements. The root-mean-square errors of 4% to 7% are within the range of previous estimates using diffuse reflectance data and are acceptable for the general extensive range of carbonate contents (i.e., 0–70 wt%) that characterize sedimentation at Leg 172 sites.

### INTRODUCTION

The record of calcium carbonate is a valuable stratigraphic and paleoenvironmental tool for the study of deep-sea sedimentation. Biogenic carbonate represents both a source and a sink in the global carbon cycle, and the interpretation of carbonate records provides insights into the temporal and spatial evolution of ocean chemistry and productivity (e.g., Mayer, 1991, and references therein). Sedimentation in the Atlantic Ocean is characterized by higher carbonate content within interglacials compared to glacials. For the Leg 172 sites, carbonate content

<sup>1</sup>Giosan, L., Flood, R.D., Grützner, J., Franz, S.-O., Poli, M.-S., and Hagen, S., 2001. High-resolution carbonate content estimated from diffuse spectral reflectance for Leg 172 sites. In Keigwin, L.D., Rio, D., Acton, G.D., and Arnold, E. (Eds.), *Proc. ODP, Sci. Results*, 172, 1–12 [Online]. Available from World Wide Web: <[http://www-odp.tamu.edu/publications/172\\_SR/VOLUME/CHAPTERS/SR172\\_06.PDF](http://www-odp.tamu.edu/publications/172_SR/VOLUME/CHAPTERS/SR172_06.PDF)>. [Cited YYYY-MM-DD]

<sup>2</sup>Marine Sciences Research Center, State University of New York at Stony Brook, Stony Brook NY 11794-5000, USA. Correspondence author:

[Liviu.Giosan@msrc.sunysb.edu](mailto:Liviu.Giosan@msrc.sunysb.edu)

<sup>3</sup>GEOMAR, Wischhofstrasse 1-3, 24148 Kiel, Federal Republic of Germany.

<sup>4</sup>Department of Geological Sciences, University of South Carolina, Columbia SC 29208, USA.

<sup>5</sup>Institute of Biology and Geology, Universitetet i Tromsø, Tromsø 9037, Norway.

Initial receipt: 20 August 1999

Acceptance: 26 July 2000

Web publication: 19 January 2001

Ms 172SR-210

pattern matching (J. Grützner et al., unpubl. data) allows the identification of climatic cycles and correlation between holes and sites.

Traditionally, the calcium carbonate content is determined on discrete samples of cored material by pressure calcimetry or coulometric techniques (e.g., Mayer, 1991, and references therein). The methods are labor intensive and destructive. In the last decade, numerous core logging devices have been developed for measuring sediment physical properties quasicontinuously, rapidly, and nondestructively. Sedimentary components, including carbonate, were estimated with various degrees of accuracy using core logging data (e.g., Mayer, 1991; Weber, 1998). The development of empirical relationships between the diffuse spectral reflectance and carbonate content on a relatively limited, representative set of sediment samples provides a rapid, high-resolution, and noninvasive alternative to direct measurement of carbonate (Balsam and Deaton, 1996; Harris et al., 1997; Ortiz et al., 1999). The matrix-dependence of sediment spectra (Balsam and Deaton, 1996) precludes the development of a general equation for the prediction of sedimentary components. The empirical relationships, however, can have a regional applicability in areas with a similar sedimentation regime (e.g., Harris et al., 1997).

Previous carbonate content estimates were derived from sediment reflectance spectra in the visible domain or extended into near-ultraviolet and near-infrared domains on either dried samples (Balsam and Deaton, 1996) or using the Oregon State University split-core analysis track on wet core surfaces (Harris et al., 1997; Ortiz et al., 1999). During most Ocean Drilling Program cruises, however, sediment reflectance has been routinely measured over the visible spectral range with a Minolta CM-2002 handheld spectrophotometer. Balsam et al. (1997) have shown that accurate spectral data can be obtained on wet cores using the Minolta system. Since the major objective of Leg 172 was to obtain a detailed history of late Neogene paleoceanography and paleoclimate in the North Atlantic, the goal of our study was to provide high-resolution, empirical predictions of carbonate content using multiple linear regression on diffuse spectral reflectance measurements.

## **METHODS**

Diffuse reflectance spectra were measured after core splitting aboard the *JOIDES Resolution* (JR) using the Minolta CM-2002 handheld spectrophotometer. The technical characteristics of Minolta spectrophotometer and the methods for acquiring the reflectance spectra are those presented by Balsam et al. (1997). The measurements were taken at intervals varying from 2 to 5 cm (Keigwin, Rio, Acton, et al., 1998). A total of 4141 carbonate measurements, including those measured on board (Keigwin, Rio, Acton, et al., 1998), were used for calibration (Table T1; S.-O. Franz and R. Tiedemann, unpubl. data; M.-S. Poli, unpubl. data; and S. Hagen et al., unpubl. data). Both raw spectra (measured from 400 to 700 nm wavelength at 10-nm intervals) as well as pretreated reflectance spectra (see below), located within 3 cm on each side of the position of the samples measured for carbonate content, were used as input for a stepwise multiple linear regression. The transformations applied to the raw spectra as pretreatments consisted of squaring and first-order derivation. Squaring reduces the nonlinearity in the relationship between the reflectance and carbonate (Harris et al., 1997). The first derivative of the raw reflectance spectrum (computed as a first-difference

---

**T1.** Calcium carbonate measurements, p. 9.

---

derivative between each pair of successive reflectance values and plotted at the midpoint of the 10-nm interval between the two values; Balsam et al. (1997) exhibits an increased variability over the initial smooth spectral curves of deep-sea sediments and therefore helps discriminate mineral-specific spectral features (Balsam and Deaton, 1996). Attempts to include magnetic susceptibility in the regression as an additional inversely correlated proxy for carbonate content did not improve the results.

Because only reflectance data were used, all regression equations were forced through the origin because no minerals can be identified when the reflectance across the spectrum falls to zero (Balsam and Deaton, 1996). Following the strategy outlined by Mix et al. (1995), the carbonate measurements made on discrete samples were initially split into calibration and verification data sets. After verification, the regression-derived calibration equations were developed using all data available.

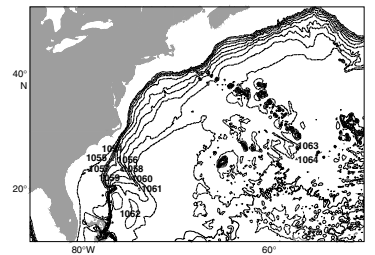
## RESULTS AND DISCUSSION

Calibration equations were developed for each site and for each lithostratigraphic unit (or subunits in the case of Site 1063) described on board the JR within each site. Carbonate distribution changes between stratigraphic units (Keigwin, Rio, Acton, et al., 1998): Unit I at Sites 1054 through 1062 on the Blake-Bahama Outer Rise (BBOR) (Fig. F1) consists of a rhythmic alternation between nannofossil-rich and clay-rich sediments and corresponds to the intensification of the 100-k.y. orbital forcing within the last 900 k.y.; Unit II and Unit III are dominated by terrigenous sediments. A similar lithostratigraphy is apparent between the Subunits IA, IB, and IC at the Bermuda Rise (BR) Site 1063 (Keigwin, Rio, Acton, et al., 1998) (Fig. F1). Additionally, opaline silica (10–30 wt%; Keigwin, Rio, Acton, et al., 1998) was detected in Subunit IA on the BR. However, the general range of variation for carbonate content is similar for all sites and units (i.e., 0–70 wt%; Fig. F2).

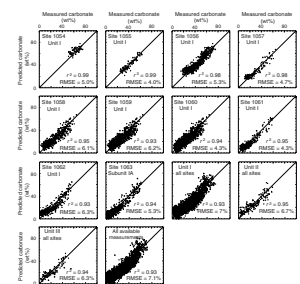
For Unit I (Subunit IA at Site 1063) we developed prediction equations for each site (Table T2; Fig. F2). However, because of the limited number of available carbonate measurements, general calibration equations for Unit II (including Subunit IB at Site 1063) and Unit III (and Subunit IC at Site 1063) included all available data from all sites (Table T2; Fig. F2). We also developed a regional general equation using all carbonate data (Table T2; Fig. F2).

The variance explained in each equation is high, as indicated by the adjusted  $r^2$ , which ranges between 0.92 and 0.99. The root-mean-square error (RMSE) of estimation is between 4% and 7%, which is within the range of previous estimates using multiple linear regression on diffuse reflectance data (Mix et al., 1995; Balsam and Deaton, 1996; Harris et al., 1997; Ortiz et al., 1999). The largest errors occurred for equations developed using data from multiple sites and for the regional equation, which also crosses lithologic boundaries (Table T2). One source of variability is the presence of detrital carbonate in glacial Atlantic sediment (e.g., Flood, 1978; Balsam and Williams, 1993). Analytical techniques do not discriminate among various carbonates that show different reflectance spectra, therefore increasing the uncertainty in the calibration. Another source of error is the mismatch between the location of the samples (i.e.,  $\leq 3$  cm) used for direct carbonate measurement and the location of the nearest reflectance measurements.

F1. Leg 172 site locations, p. 7.



F2. Measured vs. predicted carbonate, p. 8.



T2. Regression equations for carbonate content estimation, p. 10.

When compared with the 1–2 wt% errors that are typical for the direct carbonate measurement methods, the errors in our method are acceptable for the general extensive range of carbonate contents (i.e., 0–70 wt%) that characterize sedimentation at Leg 172 sites. Moreover, the relatively low RMSE for the general calibration equation indicates that regional sedimentation is remarkably uniform. However, the performance of each calibration equation with data sets other than the one for which it was developed shows that variation in mineralogical composition exists (Tables T3, T4). The deep sites on the BBOR (Sites 1058–1062) and Site 1063 on the BR are similar, with the calibration equation developed for each site performing well (i.e.,  $r^2 = >0.90$  and RMSE = <7.5%) for the other sites within the group (Tables T3, T4). There is also a similarity between Sites 1054 and 1055 drilled on the Carolina Rise, suggesting a similar mineral matrix. The equations for the sites situated at intermediate depth on the BBOR (i.e., Sites 1056 and 1057) performed equally well for both adjacent shallower or deeper sites, indicating their transitional character, but the most robust equation is the regional one.

High reflectance over the entire visual spectral range is characteristic for calcium carbonate (e.g., Gaffey, 1986). This high reflectance can be more easily distinguished in the blue end of the spectrum (400–500 nm), where increased reflectance from iron oxyhydroxides is absent. The dominant terms within the calibration equations are generally first derivatives (or their squares) of the reflectance situated between 400 and 500 nm and/or the reflectance terms (or their squares) within the middle section of the spectrum (500–600 nm). A negative term in regressions, corresponding to a reflectance value between 400 and 420 nm, most probably represents a correction for the iron oxides' absorbance band at 400–450 nm (e.g., Morris et al., 1985).

## CONCLUSIONS

Visual-domain diffuse reflectance data regularly collected aboard the JR with the Minolta CM-2002 spectrometer can be used successfully to estimate carbonate content by multiple linear regression when validated by a relatively small data set of direct measurements of carbonate content. The major advantage of this indirect estimation of carbonate content is the rapid collection of detailed, high-resolution data. One potential error source in the calibration is the mismatch in depth between the diffuse reflectance and the carbonate measurements from the validation data set. A leg-wide sampling plan that takes into account the locations of the diffuse reflectance measurements would eliminate this problem. Moreover, by coupling the sampling plan of the Minolta measurements to sampling plans for X-ray diffraction, X-ray fluorescence, and other inorganic chemistry and rock magnetism measurements, new data sets for studying the influence of sediment chemistry and mineralogy on color would be readily available, with benefits in interpreting all data sets.

## ACKNOWLEDGMENTS

We thank William Balsam, Sara Harris, and Joseph Ortiz for helpful discussions regarding the use of reflectance data in estimating mineralogical components. Suzanne O'Connell and Sara Harris are thanked for

---

T3. Correlation coefficient values for carbonate prediction equations applied to calibration data sets, p. 11.

---

---

T4. RMSE values for carbonate prediction equations applied to calibration data sets, p. 12.

---

their reviews. Thanks to Pat Malone (Lamont-Doherty Earth Observatory) for performing carbonate analyses. Many thanks to the sedimentology team for collecting the reflectance data and to the Leg 172 crew and scientific party for a successful venture at sea. This work was supported by a USSSP grant.

## REFERENCES

- Balsam, W.L., Damuth, J.E., and Schneider, R.R., 1997. Comparison of shipboard vs. shore-based spectral data from Amazon Fan cores: implications for interpreting sediment composition. *In* Flood, R.D., Piper, D.J.W., Klaus, A., and Peterson, L.C. (Eds.), *Proc. ODP, Sci. Results*, 155: College Station, TX (Ocean Drilling Program), 193–215.
- Balsam, W.L., and Deaton, B.C., 1996. Determining the composition of late Quaternary marine sediments from NUV, VIS, and NIR diffuse reflectance spectra. *Mar. Geol.*, 134:31–55.
- Balsam, W.L., and Williams, D., 1993. Transport of carbonate sediment in the western North Atlantic: evidence from oxygen and carbon isotopes. *Mar. Geol.*, 112:23–34.
- Flood, R.D., 1978. Studies of deep-sea sedimentary microtopology in the North Atlantic Ocean [Ph.D. dissert.]. Woods Hole Oceanographic Inst./Massachusetts Inst. of Technology.
- Gaffey, S.J., 1986. Spectral reflectance of carbonate minerals in the visible and near infrared (0.35 to 2.55 microns): calcite, aragonite, and dolomite. *Am. Mineral.*, 71:151–162.
- Harris, S.E., Mix, A.C., and King, T., 1997. Biogenic and terrigenous sedimentation at Ceara Rise, western tropical Atlantic, supports Pliocene–Pleistocene deep-water linkage between hemispheres. *In* Shackleton, N.J., Curry, W.B., Richter, C., and Bralower, T.J. (Eds.), *Proc. ODP, Sci. Results*, 154: College Station, TX (Ocean Drilling Program), 331–345.
- Keigwin, L.D., Rio, D., Acton, G.D., et al., 1998. *Proc. ODP, Init. Repts.*, 172: College Station, TX (Ocean Drilling Program).
- Mayer, L.A., 1991. Extraction of high-resolution carbonate data for paleoclimate reconstruction. *Nature*, 352:148–150.
- Mix, A.C., Harris, S.E., and Janecek, T.R., 1995. Estimating lithology from nonintrusive reflectance spectra: Leg 138. *In* Pisias, N.G., Mayer, L.A., Janecek, T.R., Palmer-Julson, A., and van Andel, T.H. (Eds.), *Proc. ODP, Sci. Results*, 138: College Station, TX (Ocean Drilling Program), 413–427.
- Morris, R.V., Lauer, H.V., Jr., Lawson, C.A., Gibson, E.K., Jr., Nace, G.A., and Stewart, C., 1985. Spectral and other physico-chemical properties of submicron powders of hematite, maghemite, magnetite, goethite, and lepidocrocite. *J. Geophys. Res.*, 90:3126–3144.
- Ortiz, J., Mix, A.C., Harris, S., and O’Connell, S., 1999. Diffuse spectral reflectance as a proxy for percent carbonate content in North Atlantic sediments. *Paleoceanography*, 14:171–186.
- Weber, M.E., 1998. Estimation of biogenic carbonate and opal by continuous non-destructive measurements in deep-sea sediments: application to the eastern Equatorial Pacific. *Deep-Sea Res., Part I*, 45:1955–1975.

Figure F1. Locations of sites drilled during Leg 172.

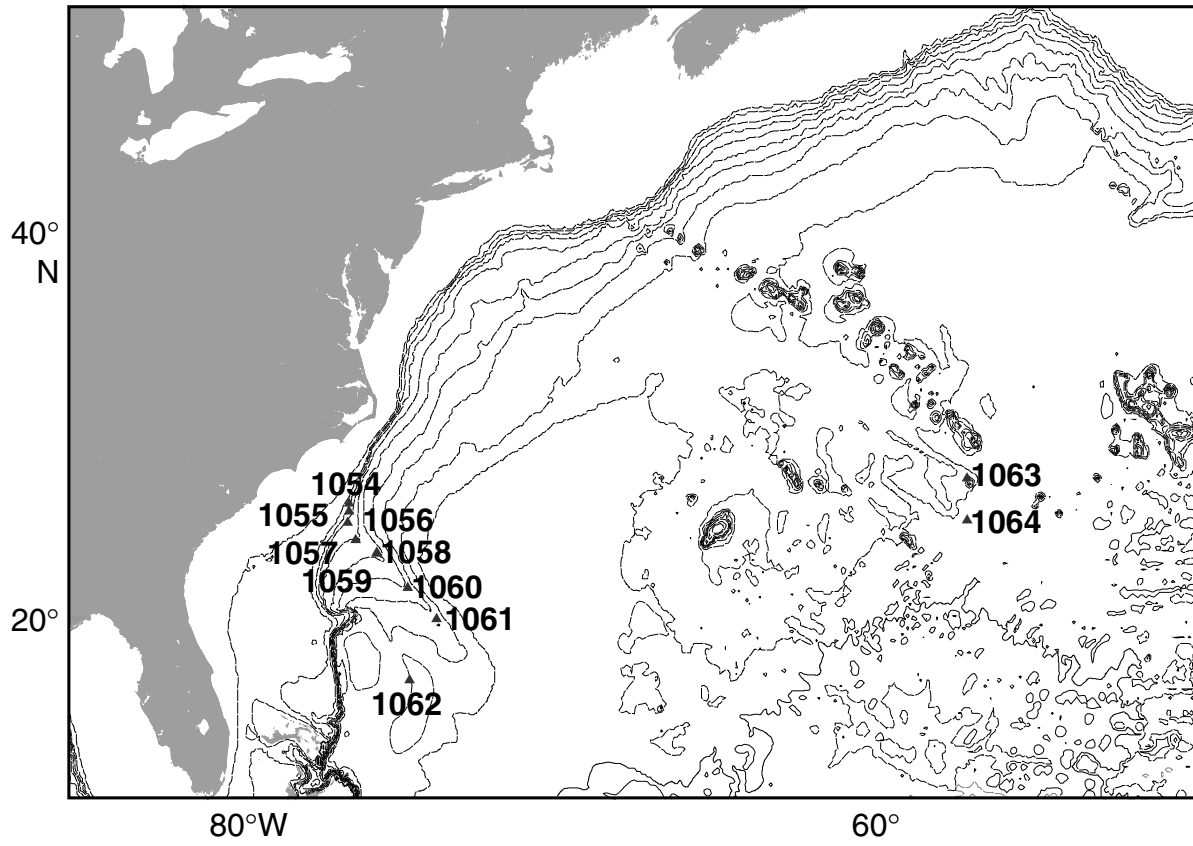
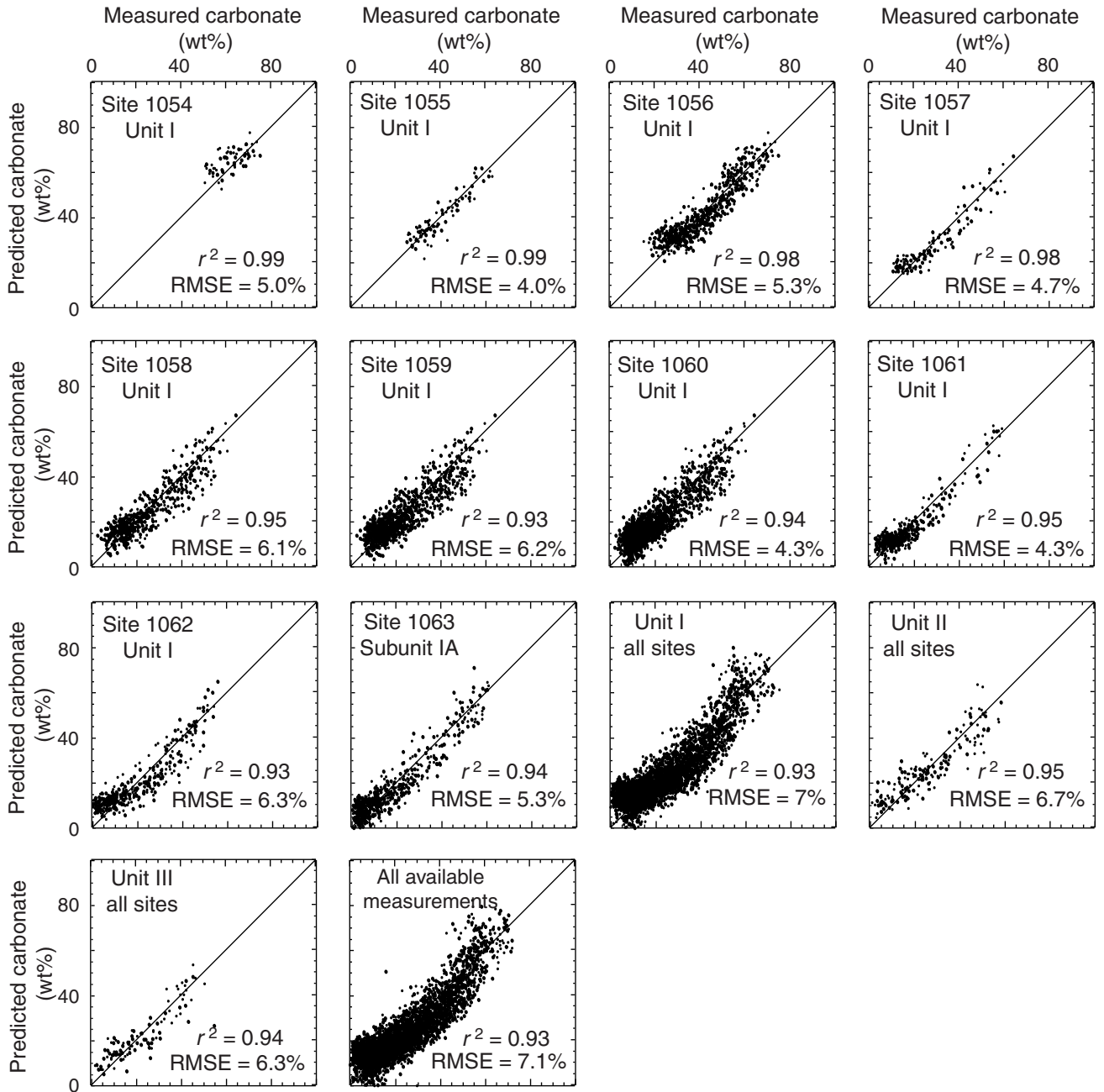


Figure F2. Measured carbonate vs. predicted carbonate and their relevant statistics for the regression equations presented in Table T2, p. 10. RMSE = root-mean-square error;  $r^2$  = correlation coefficient.



**Table T1.** Calcium carbonate measurements, Leg 172.

Core, section, interval (cm)	CaCO <sub>3</sub> (wt%)	Core, section, interval (cm)	CaCO <sub>3</sub> (wt%)
172-1057B-		5H-2, 50-52	18.57
3H-3, 94-96	12.94	172-1062F-	
3H-4, 34-36	49.46	4H-1, 24-26	33.39
3H-5, 9-21	38.10	4H-2, 24-26	10.31
3H-5, 74-76	49.65	4H-3, 92-94	7.30
3H-6, 64-36	29.44	4H-4, 54-56	39.88
3H-6, 104-106	36.70	4H-4, 122-124	14.34
3H-7, 39-41	20.73	4H-5, 94-96	12.93
4H-1, 44-46	15.45	4H-6, 120-122	28.94
4H-2, 59-61	13.92	5H-1, 55-57	38.45
4H-3, 4-16	54.44	5H-2, 61-63	3.83
4H-3, 44-46	31.60	5H-2, 139-141	46.34
4H-4, 49-51	54.48	5H-4, 41-43	49.87
4H-4, 14-106	58.68	5H-4, 143-145	3.37
4H-5, 39-41	26.69	5H-5, 85-87	20.29
4H-6, 34-36	28.71	5H-7, 25-27	3.04
4H-6, 124-126	16.54	6H-2, 51-53	47.27
5H-1, 74-76	16.39	6H-3, 47-49	1.61
5H-2, 19-21	36.15	6H-5, 15-17	20.45
5H-3, 64-66	60.61	6H-6, 127-129	31.73
5H-4, 19-21	32.29	172-1063A-	
172-1061C-		6H-1, 88-90	15.41
6H-2, 64-66	13.45	6H-2, 38-40	10.96
6H-5, 88-90	31.41	6H-3, 64-66	37.56
172-1061D-		172-1063B-	
7H-2, 105-107	7.31	6H-1, 105-107	10.51
7H-4, 48-50	23.11	6H-2, 120-122	17.22
7H-6, 72-74	48.27	6H-3, 105-107	3.43
8H-1, 80-82	8.25	6H-5, 127-129	22.77
8H-4, 28-30	19.41	6H-7, 16-18	35.35
8H-6, 140-142	7.15	7H-1, 77-79	19.58
9H-2, 12-14	6.13	7H-3, 75-77	15.82
9H-4, 42-44	55.43	7H-4, 133-135	4.27
9H-6, 132-134	34.02	7H-6, 93-95	48.16
1H-1, 122-124	32.46	8H-3, 7-9	13.69
10H-3, 7-9	57.80	8H-4, 39-41	4.45
10H-4, 132-134	7.62	8H-5, 99-101	7.41
10H-5, 57-59	18.15	8H-6, 111-113	17.62
10H-7, 51-53	8.67	9H-1, 35-37	16.98
11H-2, 27-29	6.99	9H-2, 85-87	5.93
11H-3, 127-129	5.86	9H-4, 85-87	4.68
11H-5, 83-85	32.48	9H-6, 41-43	50.29
12H-1, 111-113	55.67		
12H-4, 7-9	3.47		
12H-5, 139-141	12.55		
172-1062E-			
4H-1, 48-50	9.21		
4H-2, 68-70	9.64		

Note: These data were provided by the Marine Sciences Research Center, State University of New York at Stony Brook (measured at Lamont-Doherty Earth Observatory).

Table T2. Regression equations for carbonate content estimation, Leg 172.

Site	Unit/ Subunit	N	Adjusted $r^2$	RMSE (%)	Prediction equation – CaCO <sub>3</sub> (wt%)*
1054	I	63	0.994	4.99	$= 380.59D_{465} - 9488.62(D_{455})^2 + 494.79D_{435} + 844.46D_{655} + 18760.06(D_{695})^2 + 940.74D_{455}$
1055	I	91	0.990	4.02	$= 1.204R_{490} + 384.973D_{445}$
1056	I	594	0.983	5.32	$= 1.104R_{580} + 418.649D_{445} + 3733.452(D_{675})^2$
1057	I	127	0.977	4.74	$= 0.062(R_{610})^2 - 10.930R_{400} + 9.994R_{470}$
1058	I	434	0.949	6.10	$= 347.94D_{465} + 5681.51(D_{465})^2 + 0.03(R_{630})^2 + 304.52D_{575} + 15680.56(D_{675})^2 - 22767.19(D_{575})^2$
1059	I	518	0.932	6.17	$= 42.745D_{465} + 0.058(R_{550})^2 + 7417.036(D_{455})^2$
1060	I	618	0.941	4.27	$= -0.043(R_{550})^2 + 9367.365(D_{435})^2 + 0.093(R_{500})^2$
1061	I	421	0.950	4.32	$= 0.042(R_{530})^2 + 13009.538(D_{435})^2 - 11604.8(D_{485})^2 + 199.2D_{405}$
1062	I	353	0.933	6.30	$= 5965.94(D_{485})^2 + 0.032(R_{640})^2 - 15748.5(D_{605})^2 + 7737.974(D_{415})^2 + 192.354D_{405}$
1063	IA	629	0.944	5.27	$= 5517.618(D_{455})^2 + 679.051D_{405} + 311.074D_{595} + 0.087(R_{530})^2 - 1.504R_{400} - 7836.977(D_{405})^2$
All	I	3862	0.934	7.09	$= 603.751D_{465} + 0.056(R_{540})^2 - 0.873R_{420}$
All	II	165	0.949	6.70	$= 343.692D_{465} + 8676.303(D_{415})^2 + 766.342D_{515} - 6092.993(D_{485})^2 - 2296.044(D_{565})^2$
All	III	103	0.940	6.31	$= 809.884D_{465} - 26491.2(D_{585})^2 + 10140.34D_{655}$
All	All	4141	0.935	7.07	$= 620.267D_{465} + 0.0536(R_{540})^2 - 0.855R_{420}$

Notes: N = number of samples. Adjusted  $r^2$  = adjusted correlation coefficient. RMSE = root-mean-square error. \* = the following abbreviations are used for the regression terms: R<sub>xxx</sub> = percent reflectance at xxx nm wavelength; D<sub>yyy</sub> = the first derivative of the reflectance at yyy nm wavelength (i.e., calculated as a first difference between reflectance at [yyy + 5] nm and reflectance at [yyy - 5] nm).

**Table T3.** Compilation of correlation coefficient values for the carbonate prediction equations at each site/unit applied to each calibration data set, Leg 172.

Equation/ Data set	Unit I									Subunit IA	All	All	All	All
	1054	1055	1056	1057	1058	1059	1060	1061	1062	1063	Unit I	Unit II	Unit III	data
1054	0.99	0.98	0.98	0.97	0.97	0.96	0.95	0.95	0.95	0.94	0.97	0.98	0.98	0.98
1055	0.97	0.99	0.99	0.97	0.96	0.94	0.91	0.89	0.95	0.91	0.97	0.97	0.97	0.97
1056	0.96	0.98	0.98	0.97	0.94	0.94	0.94	0.93	0.93	0.91	0.96	0.97	0.96	0.96
1057	0.93	0.94	0.95	0.98	0.95	0.97	0.96	0.96	0.93	0.95	0.97	0.96	0.93	0.97
1058	0.89	0.89	0.90	0.94	0.95	0.94	0.93	0.93	0.91	0.89	0.94	0.92	0.92	0.94
1059	0.87	0.89	0.90	0.92	0.91	0.93	0.92	0.92	0.90	0.89	0.92	0.88	0.90	0.92
1060	0.85	0.89	0.90	0.91	0.84	0.94	0.94	0.94	0.88	0.76	0.91	0.89	0.80	0.91
1061	0.84	0.85	0.86	0.94	0.88	0.93	0.94	0.95	0.89	0.86	0.94	0.91	0.89	0.94
1062	0.82	0.82	0.84	0.92	0.77	0.91	0.90	0.89	0.93	0.93	0.91	0.88	0.76	0.91
1063	0.77	0.77	0.79	0.92	0.60	0.90	0.89	0.89	0.91	0.94	0.90	0.88	0.64	0.90
All Unit I	0.86	0.88	0.89	0.93	0.84	0.92	0.90	0.88	0.87	0.89	0.93	0.89	0.86	0.93
All Unit II	0.91	0.90	0.91	0.94	0.89	0.90	0.87	0.84	0.87	0.86	0.93	0.95	0.91	0.93
All Unit III	0.90	0.90	0.90	0.90	0.88	0.88	0.87	0.87	0.81	0.77	0.91	0.91	0.94	0.91
All data	0.86	0.88	0.89	0.92	0.84	0.92	0.90	0.87	0.86	0.89	0.95	0.89	0.86	0.94

Notes: Prediction equations (rows) are named after the site or lithostratigraphic unit for which they were developed. Calibration data sets (columns) also correspond to the site or lithostratigraphic unit from which they were measured.

**Table T4.** Compilation of RMSE percentages for the carbonate prediction equations at each site/unit applied to each calibration data set, Leg 172.

Equation/ Data set	Unit I										Subunit IA	All	All	All	All
	1054	1055	1056	1057	1058	1059	1060	1061	1062	1063	Unit I	Unit II	Unit III	data	
1054	5.47	9.38	8.87	10.50	11.00	13.00	13.40	14.60	13.50	14.70	9.93	8.44	9.41	9.85	
1055	6.76	3.99	4.03	6.88	8.64	10.20	12.10	13.70	9.12	12.60	7.33	7.15	7.07	7.34	
1056	8.73	5.54	5.31	7.62	10.00	9.89	10.20	11.00	10.90	12.40	8.38	7.76	8.05	8.24	
1057	8.30	7.50	6.80	4.70	7.25	5.59	6.11	6.22	8.30	6.90	5.28	6.53	8.09	5.27	
1058	8.82	8.79	8.41	6.75	6.06	6.78	6.93	7.25	8.11	8.97	6.72	7.76	7.48	6.73	
1059	8.57	7.74	7.63	6.54	6.97	6.22	6.68	6.92	7.55	7.85	6.59	8.13	7.46	6.63	
1060	6.77	5.82	5.66	5.32	6.97	4.43	4.26	4.45	6.05	8.61	5.18	5.93	7.84	5.21	
1061	7.71	7.55	7.21	4.79	6.71	4.96	4.61	4.31	6.44	7.20	4.89	5.80	6.47	4.91	
1062	10.30	10.20	9.80	7.06	11.70	7.38	7.64	7.97	6.27	6.58	7.31	8.46	11.80	7.35	
1063	10.60	10.60	10.20	6.27	14.10	6.97	7.31	7.20	6.82	5.25	7.09	7.76	13.28	7.15	
All Unit I	10.50	9.72	9.32	7.43	10.90	7.78	8.71	9.55	10.10	9.08	7.09	9.31	10.52	7.10	
All Unit II	8.82	9.51	9.02	7.13	9.71	9.19	10.80	11.90	10.90	10.90	7.72	6.61	9.02	7.69	
All Unit III	8.23	8.34	8.15	8.20	8.83	8.78	9.24	9.49	11.20	12.50	7.89	7.82	6.24	7.82	
All data	10.36	9.61	9.20	7.81	10.90	7.80	8.83	9.88	10.40	9.26	7.08	9.21	10.35	7.07	

Notes: RMSE = root-mean-square error. Prediction equations (rows) are named after the site or lithostratigraphic unit for which they were developed. Calibration data sets (columns) also correspond to the site or lithostratigraphic unit from which they were measured.